An Euler-Bernoulli Beam Formulation in Ordinary State-Based Peridynamic Framework

Cagan Diyaroglu, Erkan Oterkus and Selda Oterkus

Department of Naval Architecture, Ocean and Marine Engineering
University of Strathclyde, Glasgow, UK

Abstract

Every object in the world has a 3-Dimensional geometrical shape and it is usually possible to model structures in a 3-Dimensional fashion although this approach can be computationally expensive. In order to reduce computational time, the 3-Dimensional geometry can be simplified as a beam, plate or shell type of structure depending on the geometry and loading. This simplification should also be accurately reflected in the formulation which is used for the analysis. In this study, such an approach is presented by developing an Euler-Bernoulli beam formulation within ordinary-state based peridynamic framework. The equation of motion is obtained by utilizing Euler-Lagrange equations. The accuracy of the formulation is validated by considering various benchmark problems subjected to different loading and displacement/rotation boundary conditions.

Introduction

Every object in the world has a 3-Dimensional geometrical shape including the graphene material, which is generally described as a structure with a 2-Dimensional geometrical shape, since it has slight waviness in the thickness direction. From a computational point of view, it is usually possible to model structures in a 3-Dimensional fashion. However, such an approach can be computationally expensive especially considering complex structures such as an aeroplane, ship, etc. Hence, in some cases, it is essential to make reasonable assumptions, so that the 3-Dimensional geometry can be simplified as a beam, plate or shell type of structure. As a result, the computational time can be significantly reduced. In order to represent such simplifications, the formulations describing the problem of interest should be modified appropriately which is also true for peridynamics (PD), a new continuum mechanics formulation introduced by Silling (2000). As argued by dell'Isola et al. (2014a, 2014b, 2014c, 2015), the origins of PD go back to Piola's continuum formulation.

The original PD formulation was introduced for a 3-Dimensional geometrical configuration and each material point has three translational degrees-of-freedom. As mentioned earlier, for

simplified geometries, it is necessary to modify the formulation to represent simplified structural behaviour accurately. O'Grady and Foster (2014a) and O'Grady and Foster (2014b) developed non-ordinary state-based PD formulations for Euler-Bernoulli beam and Kirchoff-Love plate, respectively. Moreover, Taylor and Steigmann (2013) introduced a bond-based peridynamic plate model. Recently, Diyaroglu et al. (2015) presented PD Timoshenko beam and Mindlin plate formulations by taking into account transverse shear deformations. These formulations include not only the transverse deformation as degree-of-freedom, but also rotations of the cross-section. For slender beams, where the ratio of length to thickness must be greater than 10, i.e., $L/h>10$, transverse shear deformations can be neglected and Euler-Bernoulli beam formulation can be used. By doing this, it will be possible to reduce the total number of degrees-of-freedom in the system by half. Hence, in this study, a new ordinary state-based peridynamic model is developed and validated by considering various benchmark problems. The developed formulation can be used for the analysis of complex systems showing slender beam behaviour.

Kinematics of Euler-Bernoulli Beam in PD theory

In order represent an Euler-Bernoulli beam, it is sufficient to use a single row of material points along the beam axis, *x*, by using a meshless discretization as shown in Figure 1. In this particular case, the shape of the horizon, i.e. peridynamic influence domain, has a shape of a line. Moreover, each material point has only one degree of freedom along the *z*-axis, which is the transverse displacement, *w*.

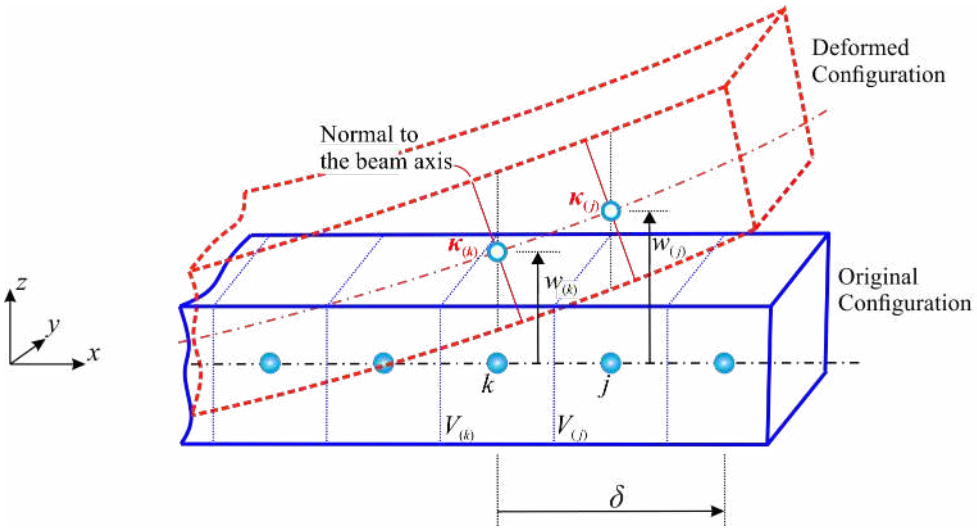

Figure 1. Kinematics of an Euler – Bernoulli beam in PD theory

By using the approach presented in Madenci and Oterkus (2014), the strain energy density function can be written in terms of micro-potentials and for material point *k*, it can be expressed as

$$W_{(k)}^{PD} = \sum_{j} \frac{1}{2}\left(\omega_{(k)(j)} + \omega_{(j)(k)}\right) V_{(j)} \tag{1}$$

where the micro-potentials $\omega_{(k)(j)}$ and $\omega_{(j)(k)}$ are the functions of transverse displacements of material points, i.e.

$$\omega_{(k)(j)} = \omega_{(k)(j)}\left(w_{(1^k)} - w_{(k)}, w_{(2^k)} - w_{(k)}, \ldots\right) \text{ and } \omega_{(j)(k)} = \omega_{(j)(k)}\left(w_{(1^j)} - w_{(j)}, w_{(2^j)} - w_{(j)}, \ldots\right).$$

The total potential energy of the beam can be obtained by summing potential energies of all material points including strain energy and energy due to external loads as

$$U^{PD} = \sum_{k} \frac{1}{2} \sum_{j} \frac{1}{2}\left(\omega_{(k)(j)}\left(w_{(1^k)} - w_{(k)}, w_{(2^k)} - w_{(k)}, \ldots\right) + \omega_{(j)(k)}\left(w_{(1^j)} - w_{(j)}, w_{(2^j)} - w_{(j)}, \ldots\right)\right) V_{(j)} V_{(k)} - \sum_{k} \hat{b}_{(k)} w_{(k)} V_{(k)} \tag{2}$$

in which $\hat{b}_{(k)}$ is the body load with a unit of "force/per unit volume" and it may represent both the transverse load, $p(x)$ and the moment load change, $\partial m(x)/\partial x$. The moment load change should be converted into a more convenient form of $\left(m_{\max.} - m_{\min.}\right)/\Delta x$, where $m_{\max.}$ and $m_{\min.}$ represent maximum and minimum moment loads, respectively, acting on a material volume. Similarly, total kinetic energy of the beam can be obtained by summing the kinetic energies of all material points as

$$T^{PD} = \frac{1}{2} \sum_{k} \rho \dot{w}_{(k)}^2 V_{(k)} \tag{3}$$

By using Eqs. (2) and (3), the Lagrangian of the system can be expressed as

$$L = T^{PD} - U^{PD} =$$

$$\frac{1}{2} \sum_{k} \rho \dot{w}_{(k)}^2 V_{(k)} - \sum_{k} \frac{1}{2} \sum_{j} \frac{1}{2}\left(\omega_{(k)(j)}\left(w_{(1^k)} - w_{(k)}, w_{(2^k)} - w_{(k)}, \ldots\right) + \omega_{(j)(k)}\left(w_{(1^j)} - w_{(j)}, w_{(2^j)} - w_{(j)}, \ldots\right)\right) V_{(j)} V_{(k)} + \sum_{i} \hat{b}_{(k)} w_{(k)} V_{(k)} \tag{4}$$

Note that the Lagrangian is only a function of transverse deflection, $w_{(k)}$. Hence, the Euler – Lagrange equation takes the form of

$$\frac{d}{dt}\frac{\partial L}{\partial \dot{w}_{(k)}} - \frac{\partial L}{\partial w_{(k)}} = 0 \tag{5}$$

Substituting Equation (4) into Equation (5) leads to

$$\rho_{(k)}\ddot{w}_{(k)} + \frac{1}{2}\sum_j\sum_i \frac{\partial \omega_{(k)(i)}}{\partial(w_{(j)} - w_{(k)})} V_{(i)} \frac{\partial(w_{(j)} - w_{(k)})}{\partial w_k} + \frac{1}{2}\sum_j\sum_i \frac{\partial \omega_{(i)(k)}}{\partial(w_{(k)} - w_{(j)})} V_{(i)} \frac{\partial(w_{(k)} - w_{(j)})}{\partial w_k} - \hat{b}_{(k)} = 0 \tag{6}$$

Moreover, the PD equation of motion for an Euler-Bernoulli beam can be expressed in a more compact form in terms of force densities, $\tilde{t}_{(k)(j)}$ and $\tilde{t}_{(j)(k)}$, as

$$\rho_{(k)}\ddot{w}_{(k)} = \sum_j (\tilde{t}_{(k)(j)} - \tilde{t}_{(j)(k)}) V_{(j)} + \hat{b}_{(k)} \tag{7}$$

where the tilde sign represents force densities arising from the bending deformation and they take the form of

$$\tilde{t}_{(k)(j)} = \frac{1}{2}\frac{1}{V_{(j)}}\sum_i \frac{\partial \omega_{(k)(i)}}{\partial(w_{(j)} - w_{(k)})} V_{(i)} = \frac{1}{V_{(j)}}\frac{\partial\left(\frac{1}{2}\sum_i \omega_{(k)(i)} V_{(i)}\right)}{\partial(w_{(j)} - w_{(k)})} \tag{8a}$$

and

$$\tilde{t}_{(j)(k)} = \frac{1}{2}\frac{1}{V_{(j)}}\sum_i \frac{\partial \omega_{(i)(k)}}{\partial(w_{(k)} - w_{(j)})} V_{(i)} = \frac{1}{V_{(j)}}\frac{\partial\left(\frac{1}{2}\sum_i \omega_{(i)(k)} V_{(i)}\right)}{\partial(w_{(k)} - w_{(j)})} \tag{8b}$$

Moreover, these force densities can also be written in terms of strain energy densities of material points, *k* and *j*, in a PD bond as

$$\tilde{t}_{(k)(j)} = \frac{1}{V_{(j)}}\frac{\partial W_{(k)}}{\partial\left(w_{(j)} - w_{(k)}\right)} \quad \text{with} \quad W_{(k)} = \frac{1}{2}\sum_i \omega_{(k)(i)} V_{(i)} \tag{9a}$$

and

$$\tilde{t}_{(j)(k)} = \frac{1}{V_{(k)}}\frac{\partial W_{(j)}}{\partial\left(w_{(k)} - w_{(j)}\right)} \quad \text{with} \quad \begin{aligned} W_{(j)} &= \frac{1}{2}\sum_i \omega_{(i)(k)} V_{(i)} \\ &= \frac{1}{2}\sum_i \omega_{(j)(i)} V_{(i)} \end{aligned} \tag{9b}$$

The strain energy densities for material points, k and j, can also be expressed by utilizing the corresponding definition from classical continuum mechanics as

$$W_{(k)} = \frac{1}{2} a \kappa_{(k)}^2 \tag{10a}$$

and

$$W_{(j)} = \frac{1}{2} a \kappa_{(j)}^2 \tag{10b}$$

where $\kappa_{(k)}$ and $\kappa_{(j)}$ represent the curvatures of material points, k and j, respectively, (Figure 1) and a is a PD parameter. The curvature functions for material points, k and j, for a bond can be defined as

$$\kappa_{(k)} = d \sum_{i^k} \frac{w_{(i^k)} - w_{(k)}}{\xi_{(i^k)(k)}^2} V_{(i^k)} \tag{11a}$$

and

$$\kappa_{(j)} = d \sum_{i^j} \frac{w_{(i^j)} - w_{(j)}}{\xi_{(i^j)(j)}^2} V_{(i^j)} \tag{11b}$$

where d is a PD parameter and it ensures that the curvature, κ, has a dimension of "1/length". Moreover, the summation sign indice, i^k, represents all material points inside the horizon of the main material point k and the indice, i^j, represents all material points inside the horizon of the family member material point j where horizon defines the influence domain of each material point. Moreover, distances between material points are defined as $\xi_{(i^k)(k)} = \left| x_{(k)} - x_{(i^k)} \right|$ and $\xi_{(i^j)(k)} = \left| x_{(k)} - x_{(i^j)} \right|$. Note that Equations (11a,b) correspond to the curvature definition in classical theory, i.e. $\kappa(x) = d^2 w / dx^2$. Substituting Equations (11a,b) into Equations (10a,b) yields the explicit expressions of strain energy densities as

$$W_{(k)} = \frac{1}{2} a d^2 \left(\sum_{i^k} \frac{w_{(i^k)} - w_{(k)}}{\xi_{(i^k)(k)}^2} V_{(i^k)} \right)^2 \tag{12a}$$

and

$$W_{(j)} = \frac{1}{2} ad^2 \left(\sum_{i^j} \frac{w_{(i^j)} - w_{(j)}}{\xi^2_{(i^j)(j)}} V_{(i^j)} \right)^2 \tag{12b}$$

The PD force densities can be rewritten by substituting Equations (12a,b) into Equations (9a,b) as

$$\tilde{t}_{(k)(j)} = \frac{ad^2}{\xi^2_{(j)(k)}} \sum_{i^k} \frac{w_{(i^k)} - w_{(k)}}{\xi^2_{(i^k)(k)}} V_{(i^k)} \tag{13a}$$

and

$$\tilde{t}_{(j)(k)} = \frac{ad^2}{\xi^2_{(j)(k)}} \sum_{i^j} \frac{w_{(i^j)} - w_{(j)}}{\xi^2_{(i^j)(j)}} V_{(i^j)} \tag{13b}$$

which can also be expressed in terms of curvature functions as

$$\tilde{t}_{(k)(j)} = \frac{ad}{\xi^2_{(j)(k)}} \kappa_{(k)} \tag{14a}$$

and

$$\tilde{t}_{(j)(k)} = \frac{ad}{\xi^2_{(j)(k)}} \kappa_{(j)} \tag{14b}$$

Note that as in the classical theory, the PD force densities occur due to bending deformation and they are functions of curvatures, $\kappa_{(k)}$ and $\kappa_{(j)}$, respectively. As shown in Figure 2, the force acting on the main material point *k* is different than the force acting on its family member, i.e. $\tilde{t}_{(k)(j)} \neq \tilde{t}_{(j)(k)}$. This is because the force function $\tilde{t}_{(k)(j)}$ is based on the displacements of material points i^k which are inside the horizon of the main material point *k* and, on the contrary, the force function $\tilde{t}_{(j)(k)}$ is based on the displacements of material points, i^j which are inside the horizon of the family member material point *j*. Therefore, the equation of motion of material point *k* given in Equation (7) is based on ordinary state-based Peridynamic theory and it can be rewritten in an open form as

$$\rho_{(k)} \ddot{w}_{(k)} = ad^2 \sum_{j=1}^{\infty} \frac{1}{\xi^2_{(j)(k)}} \left(\sum_{i^k=1}^{\infty} \frac{w_{(i^k)} - w_{(k)}}{\xi^2_{(i^k)(k)}} V_{(i^k)} - \sum_{i^j=1}^{\infty} \frac{w_{(i^j)} - w_{(j)}}{\xi^2_{(i^j)(j)}} V_{(i^j)} \right) V_{(j)} + \hat{b}_{(k)} \tag{15}$$

where the summation functions for material points j, i^k and i^j involve all family member material points inside their horizons, δ^k and δ^j.

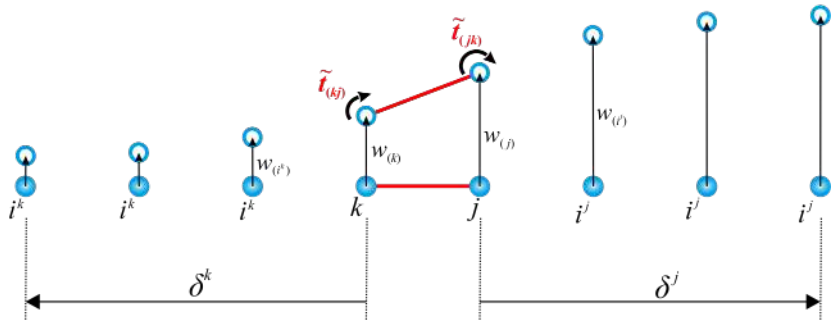

Figure 2. Force functions of a PD Euler – Bernoulli beam

In order to prove the validity of Peridynamic equation of motion (EOM) given in Equation (15), it is essential to check if its classical counterpart can be recovered in the limit of horizon sizes approaching to zero, i.e. $\delta^k \to 0$ and $\delta^j \to 0$. Therefore, the transverse displacements, $w_{(i^k)}$ and $w_{(i^j)}$, can be expressed in terms of their main material point's displacements, i.e. $w_{(k)}$ and $w_{(j)}$, respectively, by using Taylor series expansions while ignoring the higher order terms as

$$w_{(i^k)} = w_{(k)} + \xi_{(i^k)(k)} w_{(k),x} \operatorname{sgn}\left(x_{i^k} - x_k\right) + \frac{\xi^2_{(i^k)(k)}}{2} w_{(k),xx} \tag{16a}$$

and

$$w_{(i^j)} = w_{(j)} + \xi_{(i^j)(j)} w_{(j),x} \operatorname{sgn}\left(x_{i^j} - x_j\right) + \frac{\xi^2_{(i^j)(j)}}{2} w_{(j),xx} \tag{16b}$$

Substituting Equations (16a,b) in PD EOM, i.e. Equation (15), results in

$$\rho_{(k)} \ddot{w}_{(k)} = ad^2 \sum_j \frac{1}{\xi^2_{(j)(k)}} \left(\sum_{i^k=1}^{-\infty} \frac{w_{(k),xx}}{2} V_{(i^k)} + \sum_{i^k=1}^{+\infty} \frac{w_{(k),xx}}{2} V_{(i^k)} - \sum_{i^j=1}^{-\infty} \frac{w_{(j),xx}}{2} V_{(i^j)} - \sum_{i^j=1}^{+\infty} \frac{w_{(j),xx}}{2} V_{(i^j)} \right) V_{(j)} + \hat{b}_{(k)} \tag{17}$$

where the summation signs can either involve all the family members of the main material point inside the left part of the horizon or right part of the horizon. Again, if Taylor series

expansion is used for the family member material point j by disregarding the higher order terms as

$$w_{(j),xx} = w_{(k),xx} + \xi_{(j)(k)} w_{(k),xxx} \operatorname{sgn}\left(x_j - x_k\right) + \frac{\xi_{(j)(k)}^2}{2} w_{(k),xxxx} \tag{18}$$

and substituting Equation (18) into Equation (17) results in

$$\rho_{(k)} \ddot{w}_{(k)} = ad^2 \sum_{j=1}^{-\infty} \frac{1}{\xi_{(j)(k)}^2} \left(\sum_{i^j=1}^{-\infty} \frac{\xi_{(j)(k)} w_{(k),xxx} - \frac{\xi_{(j)(k)}^2}{2} w_{(k),xxxx}}{2} V_{\left(i^j\right)} + \sum_{i^j=1}^{+\infty} \frac{\xi_{(j)(k)} w_{(k),xxx} - \frac{\xi_{(j)(k)}^2}{2} w_{(k),xxxx}}{2} V_{\left(i^j\right)} \right) V_{(j)}$$

$$+ ad^2 \sum_{j=1}^{+\infty} \frac{1}{\xi_{(j)(k)}^2} \left(\sum_{i^j=1}^{-\infty} \frac{-\xi_{(j)(k)} w_{(k),xxx} - \frac{\xi_{(j)(k)}^2}{2} w_{(k),xxxx}}{2} V_{\left(i^j\right)} + \sum_{i^j=1}^{+\infty} \frac{-\xi_{(j)(k)} w_{(k),xxx} - \frac{\xi_{(j)(k)}^2}{2} w_{(k),xxxx}}{2} V_{\left(i^j\right)} \right) V_{(j)} + \hat{b}_{(k)} \tag{19}$$

After performing some algebraic manipulations, the final form of PD EOM can be obtained as

$$\rho_{(k)} \ddot{w}_{(k)} = -ad^2 \sum_{j=1}^{\infty} \left(\sum_{i=1}^{\infty} \frac{w_{(k),xxxx}}{4} V_{(i)} \right) V_{(j)} + \hat{b}_{(k)} \tag{20}$$

where i^j is replaced with i. Moreover, the infinitesimal volumes, $V_{(i)}$ and $V_{(j)}$ can be expressed for 1D beam element as $V_{(i)} = A\Delta\xi_{(i)(k)}$ and $V_{(j)} = A\Delta\xi_{(j)(k)}$, where $\Delta\xi_{(i)(k)}$ and $\Delta\xi_{(j)(k)}$ approach to differential distances, i.e. $\Delta\xi_{(i)(k)} \to d\xi''$ and $\Delta\xi_{(j)(k)} \to d\xi'$. Converting the summation terms in Equation (20) into integrations results in

$$\rho\ddot{w} = -A^2 ad^2 \int_{-\delta}^{\delta} \int_{-\delta}^{\delta} \frac{w_{,xxxx}}{4} d\xi'' d\xi' + \hat{b} \tag{21}$$

Performing the integrations in Equation (21) yields the PD EOM as

$$\rho\ddot{w} + A^2 ad^2 \delta^2 \frac{\partial^4 w}{\partial x^4} = \hat{b} \tag{22}$$

Note that, the PD EOM, given in Equation (22), has the same form as its classical counterpart for an Euler – Bernoulli beam theory, i.e.

$$\rho\ddot{w}+\frac{EI}{A}\frac{\partial^4 w}{\partial x^4}=p-\frac{\partial m}{\partial x} \tag{23}$$

As mentioned earlier, the body load, $\hat{b}$ may represent both the transverse load, p, and the moment change, $\left(m_{\max.}-m_{\min.}\right)/\Delta x$, acting on a material volume. Therefore, it can be concluded that the proposed kinetic energy, T, and strain energy density, W, expressions given in Equations (3) and (12a,b), are suitable for representation of Euler – Bernoulli beam problem.

Finally, equating the coefficients of the unknown function, w, in the PD EOM to the coefficients of that in the classical equation yields the relationships between the PD parameters, a and d, and the Young's modulus, E, and the moment of the inertia, I, as

$$a=\frac{EI}{A^3 d^2 \delta^2} \tag{24}$$

The body load can be expressed as

$$\hat{b}=p-\frac{\partial m}{\partial x} \tag{25}$$

In order to obtain a complete PD formulation, the Peridynamic material parameter, d, must also be determined. For this purpose, the curvature of a material point is compared with its classical counterpart under a simple loading condition, which can be chosen as a constant curvature, ζ. Figure 3 shows such a loading condition for a beam with a length of 2δ.

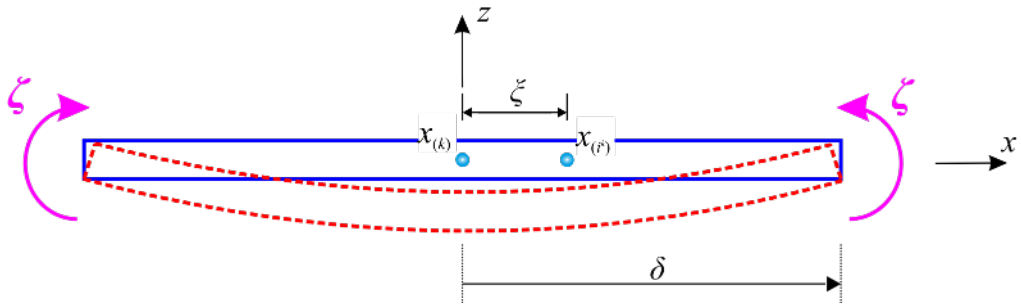

Figure 3. A beam subjected to constant curvature

In classical beam theory, the constant curvature loading is defined as

$$\kappa=\zeta=d^2w/dx^2 \tag{26}$$

Equation (26) can be solved for the specified boundary conditions which are

$$w_{(-\delta)} = w_{(\delta)} = 0 \tag{27}$$

Thus, the transverse displacement of any point on the beam axis can be defined as

$$w_{(x)} = \frac{\zeta x^2}{2} - \frac{\zeta \delta^2}{2} \quad \text{for} \quad -\delta \le x \le \delta \tag{28}$$

Here, the coordinate axis, x, is located at the centre of the beam and the main material point, k, is also at the centre with its horizon completely embedded inside the beam as shown in Figure 3. Hence, the displacement functions for material points, k and its family member point i^k, can be expressed with the help of Equation (28), as

$$w_{(k)} = -\frac{\zeta \delta^2}{2} \quad \text{and} \quad w_{(i^k)} = \frac{\zeta \xi^2}{2} - \frac{\zeta \delta^2}{2} \tag{29}$$

where $x = \xi_{(i^k)(k)} = \xi$ is used. Thus, substituting Equation (29) into Equation (11a) gives the curvature of material point k as

$$\kappa_{(k)} = d \frac{\zeta}{2} \sum_{i^k=1}^{\infty} V_{(i^k)} \tag{30}$$

Converting summation term into integration while transforming material volume as $V_{(i^k)} = A\Delta\xi_{(i^k)(k)} \to Ad\xi''$ results in

$$\kappa_{(k)} = d \frac{\zeta}{2} \int_{-\delta}^{\delta} Ad\xi'' \tag{31}$$

Performing integration and equating Equation (31) to the constant curvature, ζ, lead to the Peridynamic material parameter, d, as

$$d = \frac{1}{A\delta} \tag{32}$$

Moreover, the PD parameter, a can also be expressed in a more convenient form by substituting Equation (32) into Equation (24) as

$$a = \frac{EI}{A} \tag{33}$$

After substituting Equation (33) into Equation (10a), the strain energy density function of PD theory becomes

$$W_{(k)} = \frac{1}{2}\frac{EI}{A}\kappa_{(k)}^2 \tag{34}$$

which is equivalent to the classical theory's strain energy density expression.

Calculations For the Near Surface Material Points

Material points' stiffnesses in a beam are effected from the free surfaces or material interfaces because the Peridynamic material parameter, *d*, is derived under the assumption that the main material point, *k*, has a horizon which is completely embedded inside the beam body. On the other hand, there is no need for a correction for the bending bond constant, *a*.

In Euler – Bernoulli beam theory, the curvatures and relevant force density functions of material points which are close to the free surface are calculated numerically in a slightly different form than the given curvature equations, i.e. Equations (11a) and (11b) as well as the force density equations, i.e. Equations (13a) and (13b). The new forms of these equations are introduced with the reduced horizon sizes as explained in Appendix. Since, the horizon size is usually chosen as $\delta = 3.015\Delta x$, it is truncated at the first three material points near the free surface.

Boundary Conditions

As explained in Oterkus et al. (2015) and Madenci and Oterkus (2016), the displacement boundary conditions in PD theory can be imposed through a nonzero volume of fictitious boundary layer, R_c, as shown in Figure 4. The size of this layer is equivalent to the horizon. An external load, such as a moment or a transverse load, can be applied in the form of body loads through a layer within the actual material, R . The size of this layer can be chosen as the same size as the discretization size.

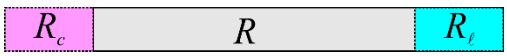

Figure 4. Application of boundary conditions in peridynamics

The application of boundary conditions in Euler – Bernoulli beam theory is slightly complicated since the theory itself only contain displacement degrees of freedom rather than rotations. In this regard, application of different types of boundary conditions is explained in detail below.

Clamped boundary condition

In order to implement clamped boundary condition, a fictitious boundary layer is introduced outside the actual material domain. The size of this layer can be equivalent to the horizon size of $\delta = 3.015\Delta x$. In classical beam theory, clamped boundary condition imposes zero displacement and zero slope on the boundary, as shown in Figure 5. In PD formulation of Euler – Bernoulli beam, this condition is achieved by enforcing mirror image of the displacement field for the first two nodes in the actual domain with respect to the first adjacent material point which is fixed. Figure 5 shows the Euler – Bernoulli beam and its discretization with incremental volumes. The red dotted line shows the deformed form of the beam axis. The displacements for the material points in the boundary region should be specified as

$$w_{(x_{i-2})} = w_{(x_{i+2})},\ w_{(x_{i-1})} = w_{(x_{i+1})} \quad \text{and} \quad w_{(x_i)} = 0 \tag{35}$$

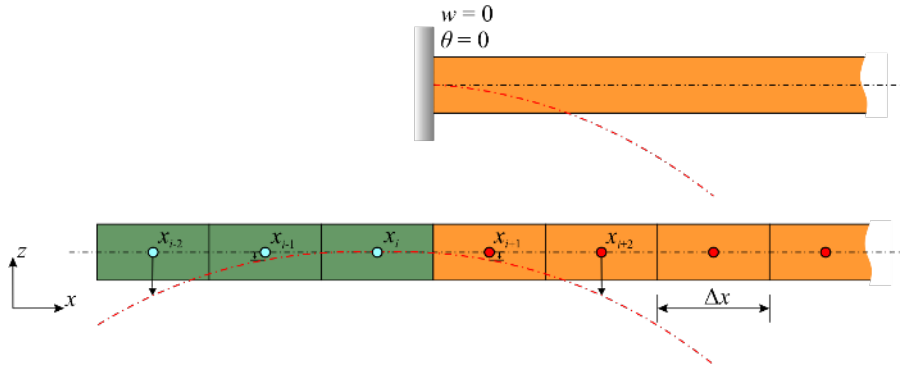

Figure 5. Clamped boundary condition

Simply supported boundary condition

In order to apply simply supported boundary condition, a fictitious boundary layer is introduced outside the actual material domain. The size of this layer can be equivalent to the horizon size of $\delta_1 = \delta_3 = 2.015\Delta x$. In classical beam theory, simply supported boundary condition imposes zero displacement and curvature on the boundary, as shown in Figure 6. In PD formulation of Euler – Bernoulli beam, this condition is achieved by enforcing negative mirror image of the displacement field for the first two nodes in the actual domain with respect to the support point. Figure 6 shows the Euler – Bernoulli beam and its PD discretization with incremental volumes. The dotted red line shows the deformed form of the beam axis. The displacements for the material points in the boundary region should be specified as

$$w_{(x_{i-2})} = -w_{(x_{i+2})} \quad \text{and} \quad w_{(x_{i-1})} = -w_{(x_{i+1})} \tag{36}$$

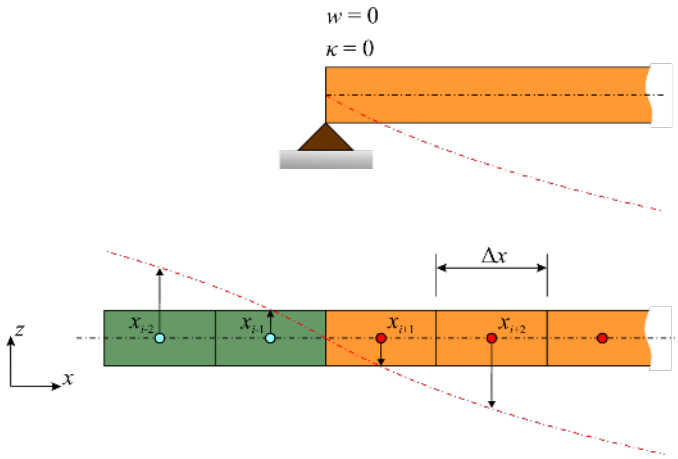

Figure 6. Simply supported boundary condition

Free boundary condition

In order to implement free boundary condition, a fictitious boundary layer is introduced outside the actual material domain. The size of this layer can be equivalent to the horizon size of $\delta = 3.015\Delta x$. In classical beam theory, free boundary condition imposes zero curvature on the boundary, as shown in Figure 7. In PD formulation of Euler – Bernoulli beam, this condition is achieved by freeing boundary points. Figure 7 shows the Euler – Bernoulli beam and its discretization with incremental volumes. Again, the dotted red line shows the deformed form of the beam axis and there is no imposed displacements for the material points in the boundary region.

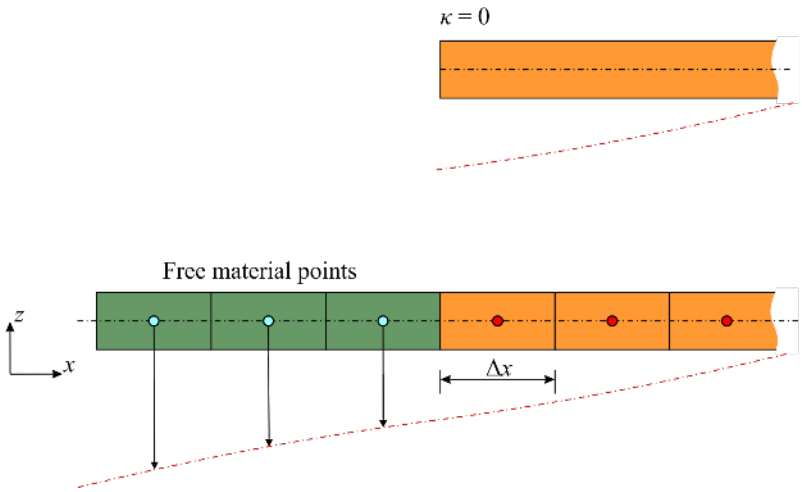

Figure 7. Free boundary condition

Numerical Solution Method

In this section, the numerical solution procedure for the EOM of Euler – Bernoulli beam theory, given in Equation (15), is presented for the problems in static equilibrium condition. In this regard, the acceleration term at the left hand side of Eq. (15) is eliminated and rearranging the terms results in

$$\sum_j \frac{ad^2}{\xi^2_{(j)(k)}} \left(\sum_i \frac{w_{(k)} - w_{(i^k)}}{\xi^2_{(i^k)(k)}} V_{(i^k)} - \sum_i \frac{w_{(j)} - w_{(i^j)}}{\xi^2_{(i^j)(j)}} V_{(i^j)} \right) V_{(j)} = \hat{b}_{(k)} \tag{37}$$

Eq. (37) can also be written in a matrix form as

$$[K]\{U\} = \{b\} \tag{38}$$

where $[K]$, $\{U\}$ and $\{b\}$ represent stiffness matrix, displacement and body force vectors, respectively. The stiffness matrix includes the Peridynamic parameters, *a* and *d*, the reference length of each bond and the material point's volume as well as the volume and the surface correction parameters. The unknown displacement vector can be determined after imposing the boundary conditions. In order to impose specified boundary constraints, the master – slave condition method can be utilized. In this method, displacement matrix can be expressed as

$$\{U\} = [T]\{\hat{U}\} \tag{39}$$

where [*T*] represents transformation matrix and $\{\hat{U}\}$ is the reduced displacement matrix with only master nodes. For example, to impose the conditions,

$$\begin{aligned} w_1 &= w_5 \\ w_2 &= w_4 \end{aligned} \tag{40}$$

which can be used to define a clamped boundary, the transformation and the reduced displacement vectors can be expressed as

$$\begin{Bmatrix} w_1 \\ w_2 \\ w_3 \\ w_4 \\ w_5 \\ . \\ . \\ w_n \end{Bmatrix} = \begin{bmatrix} 0 & 0 & 1 & 0 & 0 & 0 \\ 0 & 1 & 0 & 0 & 0 & 0 \\ 1 & 0 & 0 & 0 & 0 & 0 \\ 0 & 1 & 0 & 0 & 0 & 0 \\ 0 & 0 & 1 & 0 & 0 & 0 \\ 0 & 0 & 0 & 1 & 0 & 0 \\ 0 & 0 & 0 & 0 & 1 & 0 \\ 0 & 0 & 0 & 0 & 0 & 1 \end{bmatrix} \begin{Bmatrix} w_3 \\ w_4 \\ w_5 \\ . \\ . \\ w_n \end{Bmatrix} \quad \text{and} \quad \{U\} = [T]\{\hat{U}\} \tag{41}$$

In Equation (41), w_1 and w_2 are the slave nodes. Next, the equation of motion can be rewritten as

$$[T]^T [K][T]\{\hat{U}\} = [T]^T \{b\} \tag{42}$$

Solving Equation (42) leads to the unknown reduced displacement vector which involves only master nodes.

Numerical Results

Clamped – free beam problem

The clamped – free beam is subjected to a point load of $P = -50$ N, from the right end as shown in Figure 8. The length of the beam is $L = 1\text{m}$, with a cross-sectional area of $A = 0.01 \times 0.01$ m^2. Its Young's modulus is specified as $E = 200$ GPa. Only a single row of material (collocation) points are necessary to discretize the beam. The distance between material points is $\Delta x = 0.01$ m. Fictitious regions are created at the left and right edges with a size of $\delta = 3.015\Delta x$. The loading is imposed on only one material point, which is denoted by yellow colour in Figure 8, with a body load of $b = P/A\Delta x$.

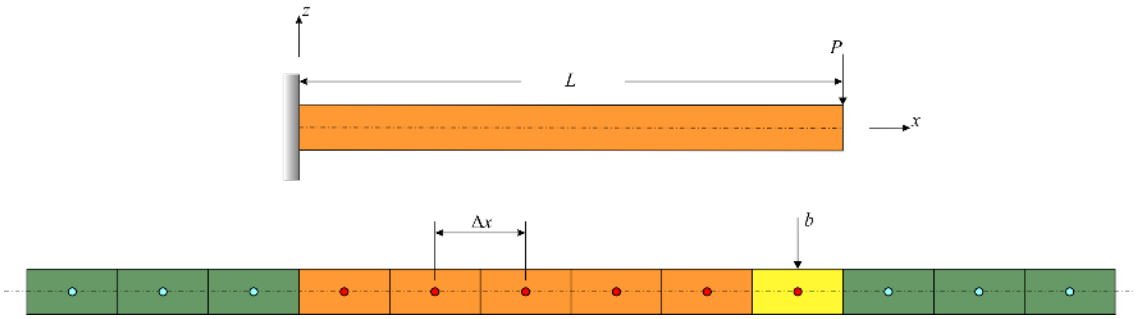

Figure 8. Clamped – free beam

The Peridynamic solution of the transverse displacement, *w*, is compared with the finite element (FE) method by using the beam element BEAM3, which is suitable for slender beams, neglects shear deformation and is available in the commercial software, ANSYS.

As depicted in Figure 9, the PD and the FE solutions agree well with each other. This verifies that the PD equation of motion can accurately capture the deformation behaviour of an Euler-Bernoulli beam for clamped-free boundary conditions.

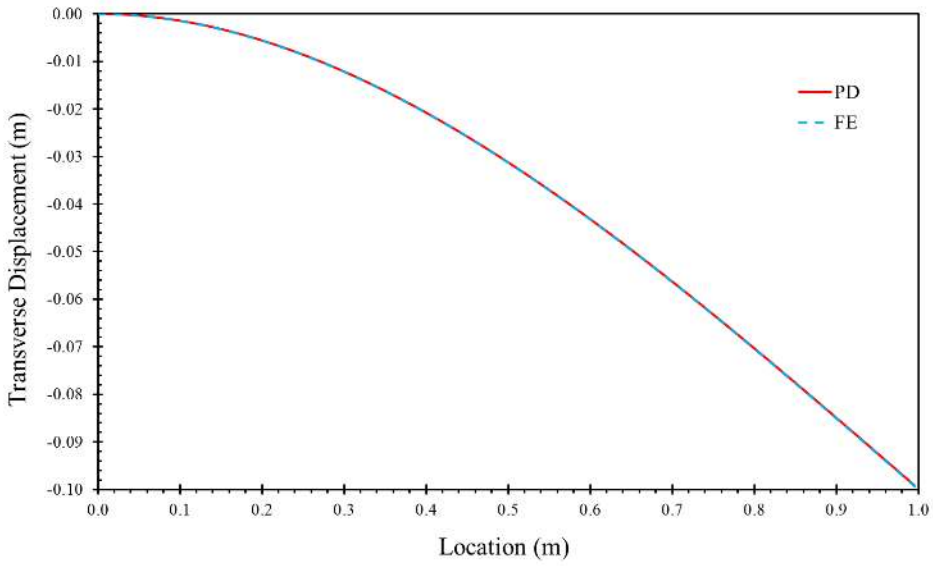

Figure 9. Displacement results of clamped – free beam

Clamped – clamped beam problem

A clamped – clamped beam is subjected to a point load of $P = -50$ N, from its center as shown in Figure 10. The length of the beam is $L = 1$m, with a cross-sectional area of $A = 0.01 \times 0.01$ m^2. Its Young's modulus is specified as $E = 200$ GPa. Only a single row of material (collocation) points are necessary to discretize the beam. The distance between material points is $\Delta x = 0.01$ m. Fictitious regions are created at the left and right edges with a size of $\delta = 3.015\Delta x$. The loading is imposed on two material points, which are denoted by yellow colour in Figure 10, as a body load of $b = P/A\Delta x$ in order to keep the symmetry.

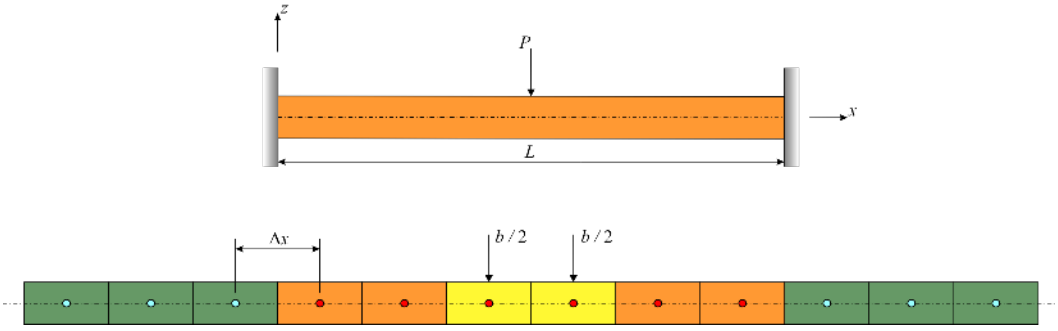

Figure 10. Clamped – clamped beam

The Peridynamic solution of the transverse displacement, *w*, is again compared with the FE method results. As depicted in Figure 11, the PD theory and the FE method results agree well with each other. This verifies that the proposed PD equation of motion can accurately capture the deformation behaviour of an Euler-Bernoulli beam for clamped-clamped boundary conditions.

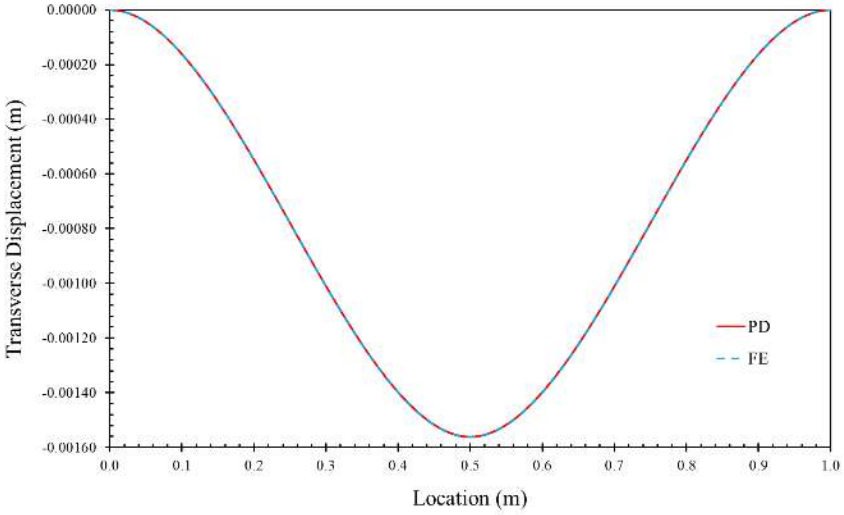

Figure 11. Displacement results of clamped – clamped beam

Simply supported – simply supported beam problem

A simply supported – simply supported beam is subjected to a point load of $P = -50$ N, from its center as shown in Figure 12. The length of the beam is $L = 1\text{m}$, with a cross-sectional area of $A = 0.01 \times 0.01$ m^2. Its Young's modulus is specified as $E = 200$ GPa. Only a single row of material (collocation) points are necessary to discretize the beam. The distance between material points is $\Delta x = 0.01$ m. Fictitious regions are created at the left and right edges with a size of $\delta_1 = \delta_3 = 2.015\Delta x$. The loading is applied to two material points, which

are denoted by yellow colour in Figure 12, with a body load of $b = P/A\Delta x$ in order to keep the symmetry.

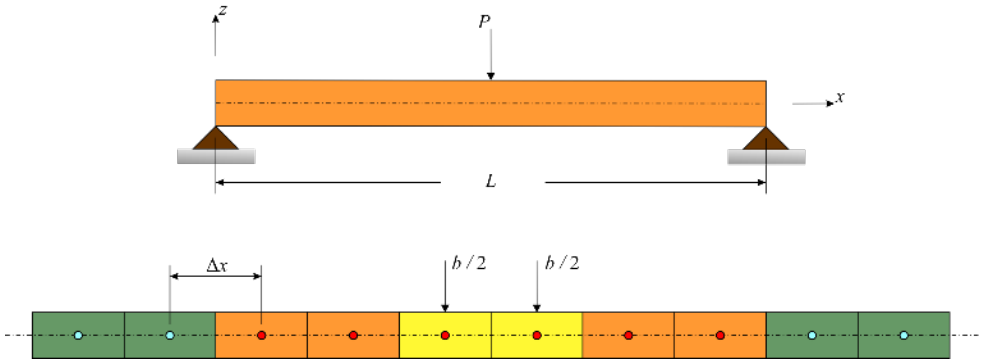

Figure 12. Simply supported – simply supported beam

The Peridynamic solution of the transverse displacement, *w*, is compared with the FE method results. As depicted in Figure 13, the PD and the FE method results agree well with each other.

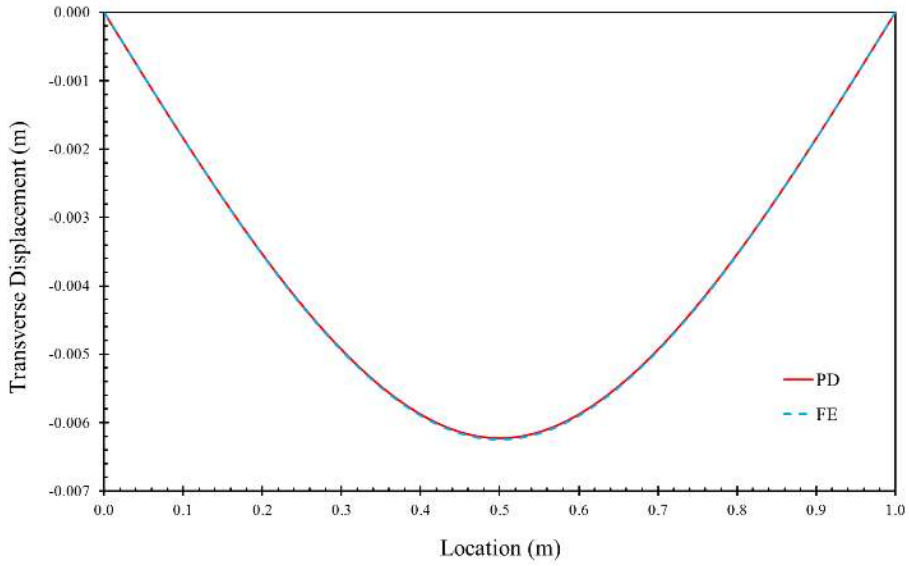

Figure 13. Displacement results of simply supported – simply supported beam

Conclusions

In this study, a new ordinary state-based peridynamic formulation for Euler-Bernolli beam is presented. The equation of motion is obtained by using the Euler-Lagrange equation. The relationships between peridynamic parameters and relevant parameters in the classical theory are established by utilizing Taylor expansion for a special case of horizon size converging to zero. The main advantage of the developed formulation is the reduction of number of degrees

of freedom for each material point by half with respect to Timoshenko beam formulation. Application of boundary conditions in peridynamics is also different from classical theory. Elegant ways of applying different types of boundary conditions including clamped, simply supported and free edge boundary conditions are explained. Various benchmark cases are considered to demonstrate the accuracy of the current formulation and boundary conditions. Remarkable agreement between peridynamic and finite element results are observed.

References

dell'Isola, F., Andreaus, U., Cazzani, A., Perugo, U., Placidi, L., Ruta, G. and Scerrato, D. "On a Debated Principle of Lagrange Analytical Mechanics and on Its Multiple Applications," The Complete Works of Gabriola Piola: Vol. I, Chapter 2, *Advanced Structured Materials*, Vol. 38, 2014a, pp. 371-590.

dell'Isola, F., Andreaus, U., Placidi, L. and Scerrato, D., "About the Fundamental Equations of the Motion of Bodies Whatsoever, As Considered Following the Natural Their Form and Constitution," Memoir of Sir Doctor Gabrio Piola, The Complete Works of Gabrio Piola: Vol. I, Chapter 1, *Advanced Structured Materials*, Vol. 38, 2014b, pp. 1-370.

dell'Isola, F., Andreaus, U. and Placidi, L., "A Still Topical Contribution of Gabrio Piola to Continuum Mechanics: The Creation of Peri-dynamics, Non-local and Higher Gradient Continuum Mechanics," The Complete Works of Gabrio Piola, Vol. I, Chapter 5, *Advanced Structured Materials*, Vol. 38, 2014c, pp. 696-750.

dell'Isola, F., Andreaus, U. and Placidi, L., "At The Origins and In the Vanguard of Peridynamics, Non-local and Higher-Gradient Continuum Mechanics: An Underestimated and Still Topical Contribution of Gabrio Piola," *Mathematics and Mechanics of Solids*, Vol. 20(8), 2015, pp. 887-928.

Diyaroglu, C., Oterkus, E., Oterkus, S. and Madenci, E., "Peridynamics for Bending of Beams and Plates with Transverse Shear Deformation," *International Journal of Solids and Structures,* Vols. 69-70, 2015, pp. 152-168.

Madenci, E. and Oterkus, E., Peridynamic Theory and Its Applications, Springer New York, New York, 2014.

Madenci, E. and Oterkus, S., "Ordinary State-based Peridynamics for Plastic Deformation According to von Mises Yield Criteria with Isotropic Hardening," *Journal of the Mechanics and Physics of Solids*, Vol. 86, 2016, pp. 192-219.

O'Grady, J., and Foster, J., "Peridynamic Beams: A Non-ordinary, State-based Model," *International Journal of Solids and Structures*, Vol. 51, No. 18, 2014, pp. 3177-3183.

O'Grady, J. and Foster, J., 2014, "Peridynamic Plates and Flat Shells: A Non-ordinary, State-based Model," *International Journal of Solids and Structures*, Vol. 51, No. 25, pp. 4572-4579.

Oterkus, S., Madenci, E. and Agwai, A., "Peridynamic Thermal Diffusion," *Journal of Computational Physics*, Vol. 265, 2014, pp. 71-96.

Silling, S. A., "Reformulation of Elasticity Theory for Discontinuities and Long-range Forces," *Journal of the Mechanics and Physics of Solids*, Vol. 48, 2000, pp. 175-209.

Taylor, M., and Steigmann, D.J., "A Two-dimensional Peridynamic Model for Thin Plates," *Mathematics and Mechanics of Solids,* Vol. 20, No. 8, 2015, pp. 998-1010.

Appendix

Curvature and force density calculations for the first material point near the free surface

For the first material point, *k*, near the free surface, the curvature can be calculated from

$$\kappa_{(k)} = d_1 \left(\frac{w_{(k)} - 4w_{(i^+)}}{2\Delta x^2} V_{(i^+)} + \frac{w_{(k)} + 2w_{(i^{++})}}{2\Delta x^2} V_{(i^{++})} \right) \tag{A1}$$

where d_1 is the modified Peridynamic material parameter and Δx is the distance between the material points. The material points i^+ and i^{++} are shown in Figure A1. In Equation (A1), the horizon size is assumed as $\delta_1 = 2.015\Delta x$ and it is used only if the material point *k* is the first point near the free surface. Note that Equation (A1) is obtained by using a finite difference formula for the second derivate since the curvature, κ, is the second derivative of the transverse displacement, *w*.

Next, the force density function can be obtained by substituting Equation (A1) into Equation (14a) as

$$t_{(k)(j)} = \frac{a d_1^2}{\xi_{(j)(k)}^2} \left(\frac{w_{(k)} - 4w_{(i^+)}}{2\Delta x^2} V_{(i^+)} + \frac{w_{(k)} + 2w_{(i^{++})}}{2\Delta x^2} V_{(i^{++})} \right) \tag{A2}$$

in which material points' volumes can take the form of $V_{(i^+)} = V_{(i^{++})} = A\Delta x$.

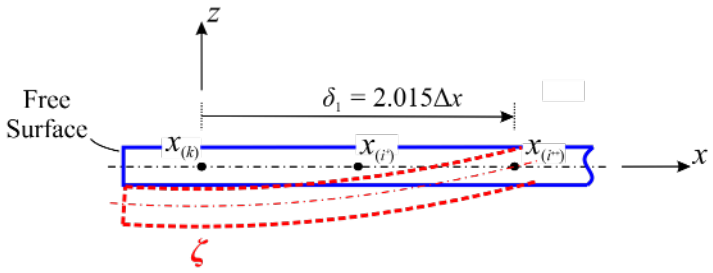

Figure A1. First main material point near the free surface

In order to determine the modified Peridynamic parameter, i.e. d_1, the beam can be subjected to a constant curvature loading, ζ, as shown in Figure A1. In this case, Equation (26) can be solved for the different boundary conditions by imposing the values of $w_{(-2\Delta x)} = w_{(2\Delta x)} = 0$. Thus, the transverse displacement of any point on the beam axis can be calculated as

$$w_{(x)} = \frac{\zeta x^2}{2} - 2\zeta\Delta x^2 \quad \text{for} \quad 0 \le x \le 2\Delta x \tag{A3}$$

From Equation (A3), the displacement functions for the material point, *k* as well as its family member points i^+ and i^{++}, can be expressed as

$$w_{(k)} = -2\zeta(\Delta x)^2,\ w_{(i^+)} = \frac{-3\zeta(\Delta x)^2}{2} \ \text{and} \ w_{(i^{++})} = 0 \tag{A4}$$

Substituting Equation (A4) into Equation (A1) leads to the curvature of material point *k* as

$$\kappa_{(k)} = \zeta d_1 A\Delta x \tag{A5}$$

Equating Equation (A5) to the constant curvature value, ζ, results in modified Peridynamic parameter, d_1, as

$$d_1 = \frac{1}{A\Delta x} \tag{A6}$$

As a summary, for the first material point near the free surface, the curvature and the force density should be calculated from Equations (A1) and (A2), respectively, while using Equation (A6) as a modified Peridynamic material parameter, d_1. Moreover, the horizon size should be assumed as $\delta_1 = 2.015\Delta x$ for this material point.

Curvature and force density calculations for the second material point near the free surface

For the second material point, *k*, near the free surface, the curvature can be calculated from Equation (11a). However, the Peridynamic material parameter *d* should be replaced with d_2 which is the modified Peridynamic parameter since the horizon size is chosen as $\delta_2 = 1.015\Delta x$ as shown in Figure A2. Thus, Equation (11a) takes the form of

$$\kappa_{(k)} = d_2 \sum_{i^k} \frac{w_{(i^k)} - w_{(k)}}{\xi^2_{(i^k)(k)}} V_{(i^k)} \tag{A7}$$

The force density function can be obtained by substituting Equation (A7) into Equation (14a) as

$$\tilde{t}_{(k)(j)} = \frac{a d_2^2}{\xi^2_{(j)(k)}} \sum_{i^k} \frac{w_{(i^k)} - w_{(k)}}{\xi^2_{(i^k)(k)}} V_{(i^k)} \tag{A8}$$

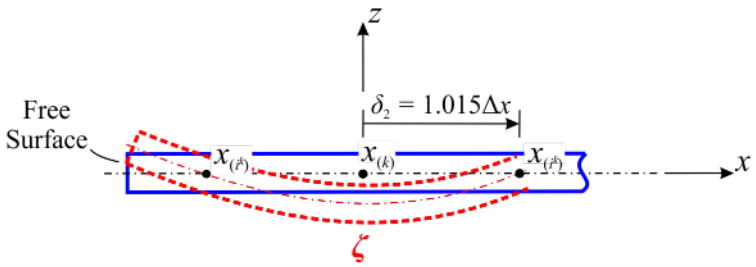

Figure A2. Second main material point near the free surface

The beam is again subjected to a constant curvature loading, ζ, shown in Figure A2, in order to determine the modified Peridynamic parameter, i.e. d_2. In this case, Equation (26) can be solved for the boundary conditions defined as $w_{(-\delta_2)} = w_{(\delta_2)} = 0$. Following similar procedures explained earlier, the modified Peridynamic parameter, d_2, can be calculated as

$$d_2 = \frac{1}{A\delta_2} \tag{A9}$$

As a summary, for the second material point near the free surface, the curvature and the force density can be calculated from Equations (A7) and (A8), respectively, while using Equation (A9) as a modified Peridynamic parameter, d_2. Moreover, the horizon size should be assumed as $\delta_2 = 1.015\Delta x$ for this material point.

Curvature and force density calculations for the third material point near the free surface

Finally, the curvature for the third material point, k, near the free surface can be calculated from Equation (11a). The modified Peridynamic parameter, d_3, can be used for the chosen horizon size of $\delta_3 = 2.015\Delta x$ as shown in Figure A3. Thus, Equation (11a) takes the form of

$$\kappa_{(k)} = d_3 \sum_{i^k} \frac{w_{(i^k)} - w_{(k)}}{\xi^2_{(i^k)(k)}} V_{(i^k)} \tag{A10}$$

The force density function can be obtained by substituting Equation (A10) into Equation (14a) as

$$\tilde{t}_{(k)(j)} = \frac{a d_3^2}{\xi^2_{(j)(k)}} \sum_{i^k} \frac{w_{(i^k)} - w_{(k)}}{\xi^2_{(i^k)(k)}} V_{(i^k)} \tag{A11}$$

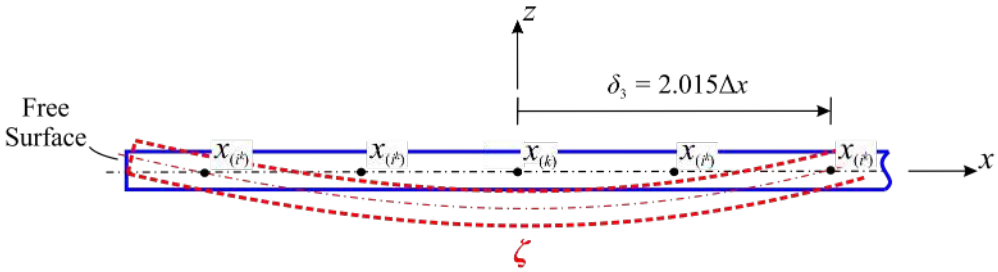

Figure A3. Third main material point near the free surface

The modified Peridynamic parameter, d_3, can be obtained by applying a constant curvature loading, ζ, to the beam as shown in Figure A3. In this case, Equation (26) can be solved for the boundary conditions of $w_{(-\delta_3)} = w_{(\delta_3)} = 0$. Following similar procedures as explained earlier, the modified Peridynamic parameter, d_3, can be calculated as

$$d_3 = \frac{1}{A\delta_3} \tag{A12}$$

As a summary, for the third material point near the free surface the curvature and the force density can be calculated from Equations (A10) and (A11), respectively, while using Equation (A12) as a modified Peridynamic parameter, d_3. Moreover, the horizon size should be assumed as $\delta_3 = 2.015\Delta x$ for this material point.